NASA Contractor Report 172215

NASA-CR-172215
19840004460

NONLINEAR DYNAMICS AND CONTROL OF A VIBRATING RECTANGULAR PLATE

John V. Shebalin

Kentron International, Inc.
Hampton, Virginia 23666

Contract NAS1-16000
October 1983

National Aeronautics and Space Administration

Langley Research Center
Hampton, Virginia 23665

TABLE OF CONTENTS

NOMENCLATURE

Z:	out-of-plane amplitude
x,y:	cartesian coordinates of plane
L:	typical length of vibration
ρ:	planar mass density
E:	Young's modulus
σ:	Poisson's ratio
h:	Plate thickness
D:	Flexural rigidity
D':	D/h
S:	Airy stress function
f:	typical frequency of vibration
u_x, u_y:	x and y component of displacement from equilibrium
∇^2:	Laplacian operator
β:	coefficient of nonlinear term
$\vec{x} = (x,y)$:	position vector

$\vec{x} = (k_x, k_y)$: wave vector

$\omega = Dk^4/\rho$: angular frequency of vibration

ϕ: phase shift

$\vec{p}, \vec{q}, \vec{r}, \vec{s}$: wave vectors

ξ: nondimensional energy

η: normalization factor

α: ratios of x-side length to y-side length of plate

$f(\vec{k}), p(\vec{k})$: forces

τ: nondimensional time

A_i, C: parameter of two-mode nonlinear system

U_i: control forces of two-mode nonlinear system

R_i: real valued amplitudes of two-mode nonlinear system

CHAPTER 1
INTRODUCTION

Linear models have had, and continue to have, great importance in the simulation and control of real processes. There are, however, some systems which are inherently nonlinear and cannot be understood fully through linear analysis alone. These nonlinear systems may be encountered, for example, in fluid mechanics, plasma physics, and structural mechanics.

Here, the need for undertaking nonlinear analysis arises from certain problems in structural mechanics. In the future, NASA expects to place into orbit large, extended and flexible structures; these structures may be expected to have oscillations large in comparison to some corresponding dimension. In this situation, system linearization through an assumption of only small oscillations is no longer possible and intrinsic nonlinearities must be retained.

A model system for studying nonlinear structural effects is found in the so called von Karman equations of nonlinear elasticity. These equations describe the dynamics of a flat plate undergoing relatively large vibrations. It is these equations which will be studied here through numerical simulation by means of a Fourier spectral transform method.

In this report the von Karman equations will be discussed as well as the numerical method for their solution. Then, preliminary results will be presented, both for a general and a reduced system. Finally, concluding remarks and possible future research directions will be given in the summary.

CHAPTER 2
EQUATIONS OF MOTIONS FOR A VIBRATING PLATE

The equations of motion for a vibrating plate follow from the equilibrium equations for such a plate and d'Alembert's Principle. The equilibrium equations for a thin plate undergoing large oscillations have been determined by A. Foppl in 1907 and T. von Karman in 1910 and are presented in standard texts on the theory of elasticity.[1,2,3]. A few preliminary remarks are needed before discussing these equations.

First, the plate will have a thickness h and the coordinate system used to describe its motion will be cartesian; when the plate is completely at rest, its neutral surface coincides with the x-y plane of the coordinate system. The out-of-plane vibrations of the plate will be described by the dependent variable $Z = Z(x,y,t)$. The following figure will be useful in discussing the equations of motion:

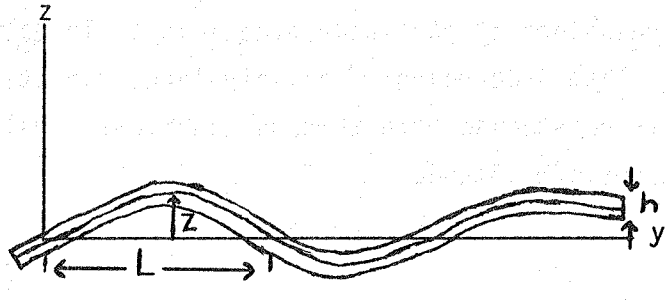

Figure 1. - Edge view of vibrating plate.

In this figure Z is a typical amplitude and L is a typical length associated with Z; also, f will denote a typical frequency associated with the vibration.

The equations of motion are

$$\rho \frac{\partial^2 Z}{\partial t^2} + D' \nabla^4 Z - \left(\frac{\partial^2 S}{\partial y^2}\frac{\partial^2 Z}{\partial x^2} + \frac{\partial^2 S}{\partial x^2}\frac{\partial^2 Z}{\partial y^2} - 2\frac{\partial^2 S}{\partial x \partial y}\frac{\partial^2 Z}{\partial x \partial y}\right) = 0 \qquad (1)$$

$$\nabla^4 S + E\left[\frac{\partial^2 Z}{\partial x^2}\frac{\partial^2 Z}{\partial y^2} - \left(\frac{\partial^2 Z}{\partial x \partial y}\right)^2\right] = 0 \qquad (2)$$

where

$$\nabla^2 = \frac{\partial^2}{\partial x^2} + \frac{\partial^2}{\partial y^2} \qquad \rho : \text{mass/unit area}$$

$$D' = \frac{Eh^2}{12(1-\sigma)^2} \qquad E: \text{Young's modulus, } \sigma : \text{Poisson's ratio}$$

S: Airy stress function : The stress tensor is related to second spatial derivatives of S.

Equations (1) and (2) are, again, derived from the Foppl-von Karman equation and d'Alembert's Principle; they form a set of coupled nonlinear equations which are accurate to a certain level of approximation. What this level is will be discussed presently.

In order to determine about how large the various terms are in the equations of motion, the following substitutions can be made in the various terms:

$$\nabla^2 \;,\; \frac{\partial^2}{\partial x^2}, \frac{\partial^2}{\partial y^2}, \frac{\partial^2}{\partial x \partial y} \;,\; \sim L^{-2}; \; \frac{\partial}{\partial t}, \sim f; \; D' \sim Eh^2$$

Using these assignments, equation (2) gives the following order of magnitude estimate: $S \sim E Z^2$. The various terms in (1) can now be given order of magnitude estimates:

$$T_1 = \rho \frac{\partial^2 Z}{\partial t^2} \sim \rho f^2 Z$$

$$T_2 = D' \nabla^4 Z \sim E L^{-4} h^2 Z$$

$$T_3 = \frac{\partial^2 S}{\partial y^2} \frac{\partial^2 Z}{\partial x^2} + \ldots \sim E L^{-4} Z^3 \qquad (3)$$

The first term, T_1, is not of immediate concern since it is driven by the other two; the ratio of the third to the second term is of interest, however, since it tells us the reasonableness of linearizing equation (1). This ratio is

$T_3/T_2 \sim Z^2/h^2$; the equation may be reasonably linearized (the third term neglected) only if $Z^2 << h^2$. If T_2 is neglected when Z^2/h^2 is not small, the frequencies and mode shapes associated with a linear solution may no longer provide an accurate dynamical description.

It was remarked earlier that although the equations of motion given by (1) and (2) were nonlinear, they were still only accurate to a certain level of approximation; this will be explained here. The equations of equilibrium from which (1) and (2) were derived can be obtained by merely replacing T_1 by $-P/h$ where P is the 'external' force applied to the plate. d'Alembert's Principle allows us to reach the equations of motion by replacing $-P$ by $\rho h Z$; thus, T_1 is really of the form

$$T_1 = \rho \frac{d^2Z}{dt^2} = \rho \frac{\partial^2 Z}{\partial t^2} + 2 \dot{u}_\alpha \frac{\partial^2 Z}{\partial X_\alpha \partial t} + \dot{u}_\alpha \dot{u}_\beta \frac{\partial^2 Z}{\partial X_\alpha \partial X_\beta} \qquad (4)$$

In (4) there is an implied summation over the repeated greek indices e.g.,

$\dot{u}_\alpha \frac{\partial}{\partial x_\alpha} = \dot{u}_1 \frac{\partial}{\partial x_1} + \dot{u}_2 \frac{\partial}{\partial x_2} = \dot{u}_x \frac{\partial}{\partial x} + \dot{u}_y \frac{\partial}{\partial y}$ where u_α are the displacements in the x and y directions. In order to get order of magnitude estimates for the terms in (4) it is necessary to get such an estimate for u_α. To do this, consider the following figure:

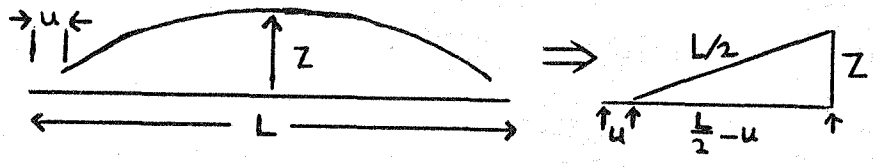

Figure 2. - Plate at rest and vibrating.

In figure 2 it is indicated that the geometry of a small section of vibrating plate can be replaced by a right triangle. This leads to an estimate of u, for Z somewhat less than L/2, of $u \sim Z^2/L$. Using this, along with the aforementioned assignments $\nabla^2 \sim L^{-2}$, etc. gives estimates of sizes of the various terms in (4):

$$T_{11} = \frac{\partial^2 Z}{\partial t^2} \sim f^2 Z$$

$$T_{12} = 2 \dot{u}_\alpha \frac{\partial^2 Z}{\partial x_\alpha \partial t} \sim f^2 L^{-2} Z^3$$

$$T_{13} = \dot{u}_\pi \dot{u}_\beta \frac{\partial^2 Z}{\partial x_\alpha \partial x_\beta} \sim f^2 L^{-4} Z^5$$

The ratio of the second to the first and the third to the first terms are

$$\frac{T_{12}}{T_{11}} \sim \frac{Z^2}{L^2} \quad , \quad \frac{T_{13}}{T_{11}} \sim \frac{Z^4}{L^4}$$

Although they will not be explicitly given here, there are also other terms of these magnitudes in (1) and (2). Thus, the equations of motion as given by (1) and (2) are valid as long as $Z^2 \ll L^2$, but are not restricted by the particular magnitude of Z^2/h^2. (If we were concerned about extremely large vibrations, i.e., $Z^2 \sim L^2$, we would have to include these neglected terms.)

In the study of control systems for large space structures at LaRC, the need to study systems for which $Z^2 > h^2$ has been recognized. Thus, equations (1) and (2) should be solved as they appear here, rather than merely solving the linearized versions alone. It would be informative to do this and then compare the nonlinear and linear solutions, both with themselves and with laboratory experiments.

There are methods for solving these nonlinear equations currently available. There are the so-called spectral methods[4] (which have been used for fluid

dynamical calculations over the last decade and are reaching a state of maturity) as well as finite difference, finite element, and Galerkin methods[5].

Finally, it is important to mention that in the one-dimensional case (e.g., the amplitude Z is a function of x, but not of y) the nonlinear term in (1) disappears. Remember that terms of relative size Z^2/L^2 have been left out of (1); the one-dimensional case does, in an exact formulation, still contain these small nonlinear terms. For our purposes, however, and to a high degree of accuracy, we may view the one-dimensional case as inherently linear while the two-dimensional case will be, in general, nonlinear.

CHAPTER 3
SPECTRAL METHOD OF SOLUTION

The equations of motion for a vibrating plate (the von Karman equations) are, again,

$$\rho \frac{\partial^2 Z}{\partial t^2} + D' \nabla^4 Z - \left(\frac{\partial^2 S}{\partial y^2} \frac{\partial^2 Z}{\partial x^2} \frac{\partial^2 S}{\partial x^2} \frac{\partial^2 Z}{\partial y^2} - 2 \frac{\partial^2 S}{\partial x \partial y} \frac{\partial^2 Z}{\partial x \partial y}\right) = f \quad (5)$$

$$\nabla^4 S + E \left[\frac{\partial^2 Z}{\partial x^2} \frac{\partial^2 Z}{\partial y^2} - \left(\frac{\partial^2 Z}{\partial x \partial y}\right)^2\right] = 0 \quad (6)$$

where

$$\nabla^2 = \frac{\partial^2}{\partial x^2} + \frac{\partial^2}{\partial y^2}$$, ρ : mass/unit area

$$D' = \frac{Eh^2}{12(1-\sigma)^2}$$ E: Young's modulus, σ : Poisson's ratio

h: plate thickness

S: Airy stress function : The stress tensor is related to second spatial derivatives of S.

f: external force applied to plate

The applicability of these equations has been discussed in the previous chapter. The basic results were: (a) that the out of plane amplitude could be considerably larger than the plate thickness (in which case the nonlinear terms in (5) become important) and (b) that the amplitude of a particular oscillatory solution was considerably less than the wavelength associated with that solution.

If the nonlinear and external force terms are neglected in (5), we have a linear equation of motion (which is sufficient in itself only for general one-dimensional motions or very small amplitude two-dimensional motions.) The linear equation has a general solution of the form

$$Z = (A\, e^{i\vec{k}\cdot\vec{x}} + B\, e^{-i\vec{k}\cdot\vec{x}} + C\, e^{\vec{k}\cdot\vec{x}} + D\, e^{-\vec{k}\cdot\vec{x}}) \cos(\omega t+\phi) \qquad (7)$$

where $\vec{x} = (x,y)$, $\vec{k} = (k_x, k_y)$, $\omega^2 = D\, k^4/\rho$ and the constants A, B, C, D, and ϕ are determined by the boundary and initial conditions. If the non-linear terms are included in (5), then an analytic solution such as (7) is, in general, not obtainable.

In the nonlinear case, an alternative method of solution is to proceed numerically. There are several numerical methods to choose from, for example, finite element, finite difference or spectral (Galerkin). Here, we will discuss the spectral method, in particular, on the (Fourier) spectral method of Orszag and Patterson[6,7].

In this spectral method the dependent quantities in the equations of motion, (5) and (6), are expressed in terms of Fourier series:

$$Z(\vec{x}, t) = \frac{1}{\sqrt{NM}} \sum_{\vec{k}} Z(\vec{k}, t)\, e^{i\vec{k}\cdot\vec{x}} \qquad (8)$$

$$S(\vec{x}, t) = \frac{1}{\sqrt{NM}} \sum_{\vec{k}} S(\vec{k}, t)\, e^{i\vec{k}\cdot\vec{x}} \qquad (9)$$

where $Z(\vec{k}, t) = Z^*(-\vec{k}, t)$ and $S(\vec{k}, t) = S^*(-\vec{k}, t)$ (*: complex conjugation), N and M are the number of points in the x and y directions, respectively; the summation limits will be discussed in Chapter 4. Whether we are discussing physical variables $Z(\vec{x})$, $S(\vec{x})$ or Fourier modes $Z(\vec{k})$, $S(\vec{k})$ is determined by their respective arguments (often the time argument will be omitted.) This choice implies that we are imposing periodic boundary conditions; B.C.'s can be discontinuous and Lanczos' Tau method can handle arbitrary B.C.'s[8].

Notice that these boundary conditions keep the trigonometric spatial eigenfunctions of the linear solution (7) while eliminating the hyperbolic ones, also in (7), from the nonlinear solutions (8) and (9). This is not a fundamental limitation since the trigonometric functions still provide a complete orthogonal basis.

The time dependence of $Z(\vec{x}, t)$ and $S(\vec{x}, t)$ is now contained in the time dependence of the Fourier coefficients $Z(\vec{k}, t)$ and $S(\vec{k}, t)$. The equations which describe the time evolution of the Fourier coefficients are determined by substituting (8) and (9) into (5) and (6); after some algebraic manipulation we have

$$\rho \frac{d^2 Z(\vec{k}, t)}{dt^2} + D' k^4 Z(\vec{k}, t) - \frac{1}{\sqrt{NM}} \sum_{\substack{\vec{p} \\ \vec{p}+\vec{q}}} \left|\vec{p} \times \vec{q}\right|^2 Z(\vec{p}, t)\, S(\vec{q}, t) = f(\vec{k}, t) \tag{10}$$

$$S(\vec{q}, t) = -\frac{E}{2q^4} \frac{1}{\sqrt{NM}} \sum_{\substack{\vec{q} \\ \vec{r}+\vec{s}}} \left|\vec{r} \times \vec{s}\right|^2 Z(\vec{r}, t)\, Z(\vec{s}, t) \tag{11}$$

Here $f(\vec{k}, t)$ is the $\vec{k}$ - Fourier mode coefficient of the external force and all $\vec{k} = 0$ coefficients are omitted from the solution. (The components of all the modal vectors $\vec{k}$, $\vec{p}$, $\vec{q}$, $\vec{r}$, and $\vec{s}$ appearing in (8), (9), (10), and (11) are integers, while the components of $\vec{x}$ in (8) and (9) take values between 0 and 2π.)

In the Orszag-Patterson spectral method, an appropriate time-differencing scheme is chosen to advance $Z(\vec{k}, t)$ in (10) forward in time. The essence of the method is not to solve for the nonlinear terms in (10) and (11) by simply summing them in $\vec{k}$-space (which takes a very long time), but instead the method finds the coefficients of the derivatives of $S(\vec{x})$ and $Z(\vec{x})$, uses an FFT (Fast Fourier Transform) to transform to $\vec{x}$ - space, forms the nonlinear terms of (5) and (6) there, then on a discrete grid of points, say N x M, where N and M are powers

of two. The x and y components of $\vec{x}$ take on the values $x_n = 2\pi\ n/N$ and $y_m = 2\pi\ m/M$ $0 \leq n \leq N-1$ and $0 \leq m \leq M-1$). The ratio in speed between the transform method and the direct sum evaluation is (logN)/N where N is also the number of distinct k_x or k_y values (i.e., the number of grid points in $\vec{x}$ - space and $\vec{k}$ - space are equal). Another important part of the method is to properly de-alias the nonlinear coefficients determined by the transform technique; this is discussed by Orszag[6], and Patterson and Orszag[7].

The purpose of this chapter has been to briefly describe the Orszag-Patterson spectral method as applied to the problem of nonlinear vibrations of a thin plate. The method can be used to study the importance of nonlinearities, particularly as the mean amplitude to plate thickness ratio is increased. This could demonstrate the need to more closely consider nonlinear effects in our attempts to understand and control the dynamics of large space structures. In the following chapters the implementation of this method and some preliminary results will be discussed.

CHAPTER 4

SPECTRAL EQUATIONS: FURTHER CONSIDERATIONS

The spectral equations developed in the last chapter can be put into a nondimensional form suitable for studying the nonlinear vibrations of a rectangular plate. The end result of doing this is shown in Figure 3; it will now be assumed that the number of points in the x and y directions will be the same and equal to N.

The equations in Figure 3 can be consolidated to eliminate the Airy stress function (i.e., its Fourier coefficients). The result of this action is presented in Figure 4a; the coefficient of the cubic nonlinear term has been explicitly symmetrized. The reason for this is the following: First, the time dependent equation in Figure 4a is multiplied by $Z^*(\vec{k}, t)$ and the resulting equation is added to its complete conjugate; then, using the fact that $N(\vec{k}, \vec{p}, \vec{r}, \vec{s})$ is completely symmetric in its arguments allows the time dependent equations in Figure 4b to be arrived at.

As is evident in the equation for $d\xi/d\tau$ in Figure 4b, in the absence of an applied force, the quantity ξ is constant (but only for an infinite Fourier expansion). This conserved quantity ξ is the energy of the vibrating plate; the term with coefficient β is the 'nonlinear' contribution; if $\beta = 0$, then $\xi = \xi_L$ is the 'linear energy'. There does not appear to be any other constant of the motion, as is the case in analogous representations of fluid and magneto-fluid systems.[9]

The behavior of the energy for a system represented by a truncated (finite) Fourier representation will be examined in the numerical example of the next chapter. Let us conclude the present chapter with some remarks concerning the contribution of the $\vec{k} = 0$ modes (coefficients) and on the statistical nature of the nonlinear dynamics.

Careful consideration of the form of $N(\vec{k}, \vec{p}, \vec{r}, \vec{s})$ shows that as $\vec{k} \to 0$, $N(...) \to 0$, regardless of the values of $\vec{p}$, $\vec{r}$, and $\vec{s}$. Thus, the $\vec{k} = 0$ Fourier coefficient has no effect on the dynamics of the plate and corresponds only to

the overall velocity of the chosen inertial reference frame. In the numerical work that follows, the zero mode coefficient will always be set equal to zero.

As in the case of nonlinear fluid systems, the presence of nonlinear terms introduces random and perhaps chaotic behavior into the time evolution of the Fourier coefficients. This randomness may be expected to manifest itself as a short correlation and autocorrelation time of the Fourier coefficients; this, in turn, allows for a statistical description of the dynamics (elastodynamic turbulence). This description can be effected through the use of a canonical (Gibbs) distribution[10] where the distribution function is

$$D(\xi) = \frac{\exp(-\alpha\xi)}{\eta} \tag{12}$$

Here α is a parameter (inverse temperature) which is chosen so that $D(\xi)$ is an extremum for $\xi = \bar{\xi}$, the actual energy of the system. The quantity η is a normalizing factor:

$$\eta = \int \exp(-\alpha\xi) \prod_{\vec{k}} d\, Z_R(\vec{k})\, d\, V_R(\vec{k})\, d\, Z_I(\vec{k})\, d\, V_I(\vec{k}) \tag{13}$$

where $Z_{R,I}(\vec{k})$ and $V_{R,I}(\vec{k}) = d\, Z_{R,I}(\vec{k})/d\tau$ are the independent coordinates of the statistical phase space ($Z_{R,I}(\vec{k})$: real, imaginary parts of $Z(\vec{k})$).

In fluid dynamical systems a similar statistical description can be utilized because constants of the motion remain constant even when the Fourier series are finite, as in the case in any numerical simulation.[9] Such is not the situation for any finite expansion of an elastodynamic system, however, although certain model systems can be developed in which the energy remains constant even with a finite number of modes. This topic will be touched upon again in the following chapters.

Fig. 3 Nondimensional Spectral Form of the von Karman Equations

$$\frac{d^2(Z\vec{k},t)}{d\tau^2} + \omega^2\,(\vec{k},\alpha)\; Z(\vec{k},t) + \frac{\beta}{N} \sum_{\vec{k}=\vec{p}+\vec{q}} \left|\vec{p}x\vec{q}\right|^2 Z(\vec{p},t)\; S(\vec{q},t) = P(\vec{k})$$

$$S(\vec{q},t) = \frac{q^{-4}}{N} \sum_{\vec{q}=\vec{r}+\vec{s}} \left|\vec{r}x\vec{s}\right|^2 Z(\vec{r},t)\; Z(\vec{s},t)$$

$$\omega(k,\alpha) = k_x^2 + \alpha^2 k_y^2 \qquad \beta = 6\,\alpha^4\,(1-\sigma^2)\,\frac{Z_o^2}{h^2}$$

Edge lengths: $L_x = L$, $L_y = L/\alpha$ $\qquad t = \left[\frac{L}{2\pi}\right]^2 \sqrt{\frac{\rho}{D'}}\,\tau$

Z_o = RMS vibrational amplitude $\qquad P(\vec{k}) = \frac{(L/2\pi)^4}{Z_o h\, D'}\, f(\vec{k})$

E: Young's Modulus $\qquad \sigma$: Poisson's ratio $\qquad D' = \frac{E\,h^2}{12\,(1-\sigma^2)}$

ρ: density $\qquad$ h: plate thickness

$P(\vec{k})$: Fourier coefficients of nondimensional force

Fig. 4a Consolidated Equations of Motion

$$\frac{d^2 Z(\vec{k},\tau)}{d\tau^2} + \omega^2(\vec{k},\alpha)\, Z(\vec{k},\tau) + \frac{\beta}{N^2} \sum_{\vec{p},\vec{r},\vec{s}} N(\vec{k},\vec{p},\vec{r},\vec{s},)\, Z^*(\vec{p})\, Z^*(\vec{r})\, Z^*(\vec{s}) = P(\vec{k})$$

$$N(\vec{k},\vec{p},\vec{r},\vec{s}) = \frac{1}{3}\left[\frac{|\vec{k}x\vec{p}|^2\,|\vec{r}x\vec{s}|^2}{|\vec{r}+\vec{s}|^4} + \frac{|\vec{k}x\vec{r}|^2\,|\vec{p}x\vec{s}|^2}{|\vec{p}+\vec{s}|^4} + \frac{|\vec{k}x\vec{s}|^2\,|\vec{p}x\vec{r}|^2}{|\vec{r}+\vec{p}|^4}\right]\delta^2(\vec{k}+\vec{p}+\vec{r}+\vec{s})$$

$$\delta^2(\vec{q}) = \begin{cases} 0, & |\vec{q}| \neq 0 \\ 1, & |\vec{q}| = 0 \end{cases}$$

Fig. 4b. Constant of the Motion: the Energy

$$\xi = \frac{1}{2}\sum_{\vec{k}}\left[\left|\frac{d\,Z(\vec{k},\tau)}{d\tau}\right|^2 + \omega^2(\vec{k},\alpha)\,\left|Z(\vec{k},\tau)\right|^2\right] + \frac{\beta}{4N^2} \sum_{\substack{\vec{k},\vec{p} \\ \vec{r},\vec{s}}} N(\vec{k},\vec{p},\vec{r},\vec{s})\, Z(\vec{k})Z(\vec{p})Z(\vec{r})Z(\vec{s})$$

$$\frac{d\xi}{d\tau} = \frac{1}{2}\sum_{\vec{k}}\left[\frac{dZ^*(\vec{k})}{d\tau} P(\vec{k}) + \frac{dZ(\vec{k})}{d\tau} P^*(\vec{k})\right]$$

CHAPTER 5
NUMERICAL SIMULATION

The numerical solution of the nonlinear von Karman equations has attracted a good deal of effort since their inception, as is evidenced by a survey of the open literature. Although spectral (Galerkin) methods seem to be widely applied, the efforts usually end in a linearization of the problem. An example is found in the article by Crawford and Atluri[11] entitled "Non-linear Vibration of a Flat Plate with Initial Stress". Crawford and Atluri present a solution by means of Galerkin approximation of the von Karman equations using the (linear) eigenfunctions appropriate for simply supported boundary conditions (two-dimensional sine series). They specialize to a problem containing only four modes (i.e., four independent sine series coefficients) and use a perturbation technique called "multiple time scaling" to solve the nonlinear ordinary differential equations for the sine series coefficients. They then show that their results are commensurate with prior perturbative analysis.

The intent here is to get away from perturbative analysis, wherein one method may easily be consistent with another, and present an alternative approach. This new approach is the Fourier spectral transform method discussed in Chapter Three. In this chapter, the numerical implementation of that method will be discussed. In particular, pertinent computational details will be considered, some preliminary results presented and practical limits on computer resource utilization will be given.

In order to create a computer code to simulate nonlinear dynamics using a Fourier spectral transform method, some essential features must be incorporated. First, there has to be a computer system available suited to intensive vector computation. At the NASA Langley Research Center, the CDC Cyber 203 (STAR) is such a machine (although it does have its inherent limitations--to be considered shortly). Next, there must be a reasonably quick and efficient Fast Fourier Transform (FFT) subroutine resident on the system (the Cyber 203 mathematics library contains the appropriate routine: Q4FFT2DR). The FFT subroutine is important because a majority of the computational time is spent performing transforms.

In the computer code, two important considerations are the time integration scheme and the de-aliasing procedure. In the preliminary code developed here, a second order 'two step' method[12] was utilized; this second order method was used rather than a higher order one so as to reduce the number of arrays needed. A de-aliasing procedure is needed because the nonlinear interaction, by its nature, feeds energy into both higher and lower order modes from those modes which have been initially excited. Thus, when FFT's are performed at each time step, it is possible to get aliased values for those modal coefficient which are being retained. This problem is circumvented by either performing 2N point transforms and keeping only the first N (or less) coefficients, or by using the advanced methods of Patterson and Orszag[6,7]; in this preliminary development the first procedure was used. Specifically, only those modes $Z(\vec{k})$ $w|\vec{k}| = k \leq K$ were retained; all modes outside the circular region defined by $k = K$ were reset to zero after each forward FFT.

As has been mentioned, the numerical technique used here has been effectively utilized to study problems in nonlinear fluid dynamics .[9] In these fluid applications the modal dynamic equations contain quadratic non-linearities, while in the elasto-dynamic case the nonlinearities are cubic. Another essential difference is that the fluid equations contain at most second order spatial derivatives while in the von Karman equations there is the biharmonic term, which is of fourth order. Therefore, if K is the largest wave vector magnitude in both the fluid and elastodynamic simulations, then the time step sizes scale as K^{-2} and K^{-4}, respectively, in these simulations; thus, while numerical simulations of fluid turbulence (nonlinear dynamics) to a certain (moderate) level of resolution may currently be feasible, the same level cannot be reached in elasto-turbulence simulations (unless a huge computer resource investment is made).

In the preliminary testing and evaluation of the transform code for the nonlinear von Karman equations the plate was represented by a grid of 16 x 16 points. The k-space cutoff was K=4; the dimensionless time step size was $(2048)^{-1}$, as any lower values allowed instabilities to grow. The initial conditions established for the Fourier coefficients $F(\vec{k},t)$ were $|F(\vec{k},0)| \sim \exp[(|\vec{k}|^2 - \bar{k}^2)/2s^2]$ where $\bar{k} = 2$ and the standard derivation was $s = 2$. The phases of the coefficients were chosen randomly and the overall energy was

normalized so that the 'linear' part ξ_L was one (i.e., that part of the energy ξ in Fig. 4b which remains when $\beta = 0$).

With these initial conditions the code was run with $\beta = 0$ (linear) and $\beta = 256$ (nonlinear). For $\beta = 0$ the energy in each mode remained constant during the time evolution of the motion (as expected.) For $\beta = 256$ modal energy did not remain constant and some modes were preferentially enhanced; this is illustrated in the sequence of Figure 5. Figure 5a is the linear part of the modal energies $\xi_L(\vec{k})$ at $t = 0$ (for $\beta = 0$ this energy distribution did not change with time). Figures 5 b and c show the transferral of energy for $\beta = 256$: energy in the mode $\vec{k} = (3,0)$ and $(-3,0)$ is augmented by nonlinear processes.

For a 1 cm thick square aluminum plate of side length 3 meters, the time of evolution shown in Figure 5 is 0.86 seconds; for a side length of 30 meters, this time becomes 86 seconds. The frequencies corresponding to these two cases are, for a side length of 3 meters, lowest ($|\vec{k}| = 1$): 11.56 Hz and augmented ($\vec{k} = (3,0)$): 105 Hz; for a side length of 30 meters, these become, lowest: 0.116 Hz and augmented: 1.05 Hz. There were no specific boundary conditions imposed; this was a 'homogeneous' elasto-turbulent simulation.

The presence of terms of order K^4 in modal von Karman equations (Figure 3) requires the investment of relatively large amounts of computer time. Table 1 presents some pertinent parameters for a typical low resolution run.

Table 1. Computational Parameters

Grid Size:	16 x 16
k-space cutoff:	K = 4
Total time:	$\tau = 100$
STAR cpu-sec/time step:	0.048 sec
Total cpu time:	2.78 hours
Number of retained modes:	50

As can be seen from Table 1, a good bit of time must be spent to perform a nonlinear elastodynamic simulation. So much time that the resources available

for this purpose were quickly expended, while interesting parts of the simulation remained untouched. In Figure 6 is a comparison of the behavior of the total energy ξ and the linear energy ξ_L between times $\tau = 0$ to 120. Here, it is evident that the total energy is not constant, as would be the case if an infinite number of modes could have been utilizied; instead, the energy falls by about 1% of its initial value. This 1% can be thought of as 'heat' loss: energy has been cascaded over the $|\vec{k}| = K$ cutoff and is no longer dynamically useful. Note that the nonlinear contribution to the energy, $\xi_N = \xi - \xi_L$, also feeds the linear energy and causes it to rise temporarily (although the total energy ξ monotonically decreases).

The code described herein is a fully nonlinear implementation of the von Karman equations, subject only to discretization error. If the computer resources are available, there are many applications which can be profitably studied, including flutter analysis, large space structure (LSS) dynamics and non-linear control; appropriate boundary conditions can be applied using Lanczos' Tau method. However, because the necessary resources are not, at present, available, a multi-mode, high resolution simulation is not feasible. This forces us to use a low-resolution model in which only a few modes are present. Such a model will be studied in the next chapter: the nonlinear dynamics of a von Karman system restricted to two modes will be investigated.

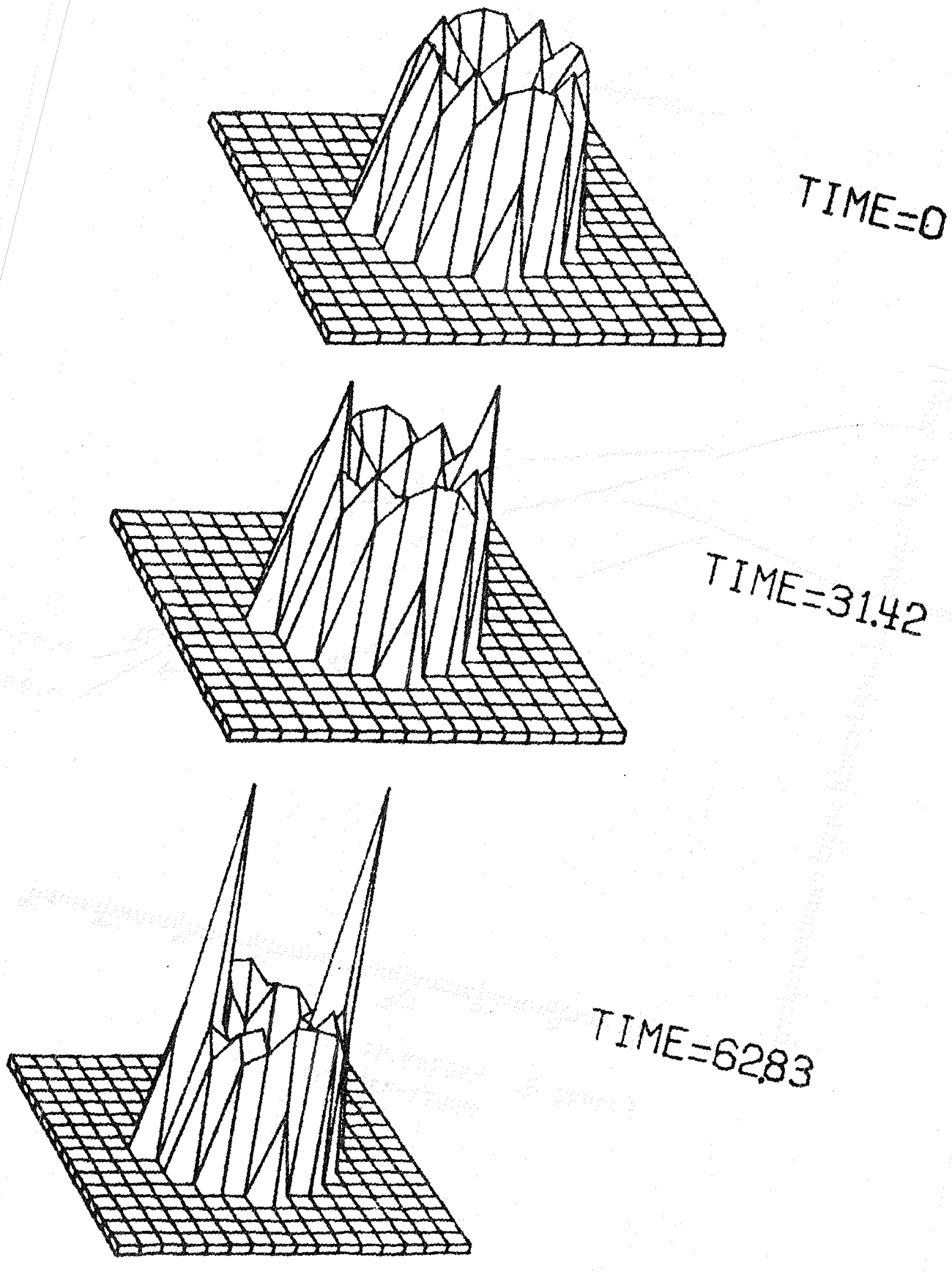

FIGURE 5. TIME EVOLUTION OF LINEAR POWER SPECTRUM.

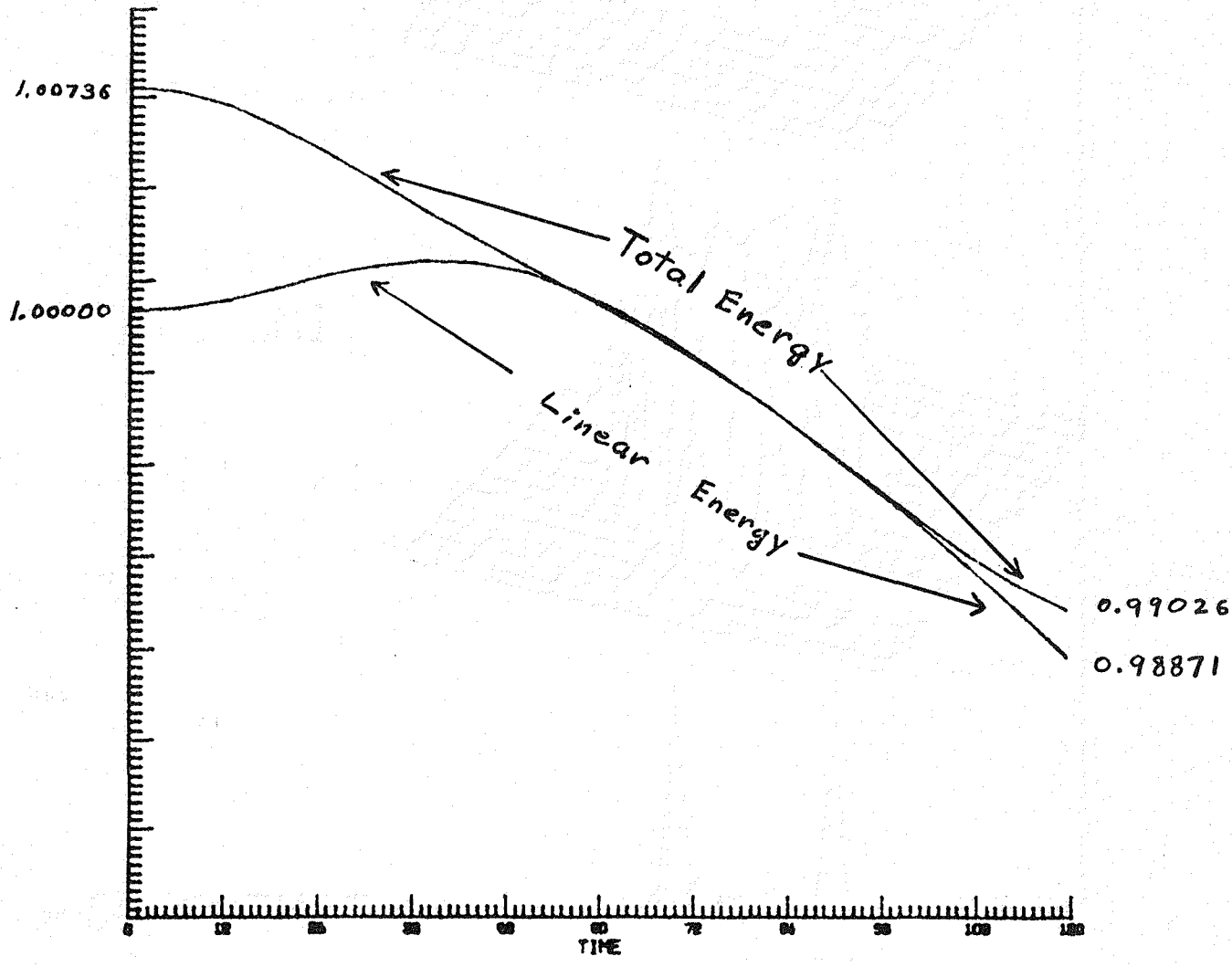

FIGURE 6. ENERGY VS TIME FOR A MULTI-MODE SYSTEM.

CHAPTER 6

DYNAMICS AND CONTROL OF A MINIMAL NONLINEAR SYSTEM

Dynamics

The results of the previous chapter have shown that if a truncated Fourier representation is used to describe the amplitude $Z(\vec{x}, t)$, and if the retained Fourier modes are initially arbitrarily excited, then the energy of the model system is not necessarily conserved. These results also illustrated the high computational cost incurred when retaining even a moderate number of Fourier coefficients. Since the purpose of this report is to gain a perspective on the control of a nonlinear elastic system, it would be useful to have a model numerical system which was inexpensive to run and in which numerical dissipation did not cloud the effects of the control scheme under study. Just such a model system will be discussed here.

Consider the modal equations represented in Figure 4a; suppose that there are only two independent Fourier modes initially excited: $Z_1 = Z(\vec{k}_1, t)$ and $Z_2 = Z(\vec{k}_2, \tau)$ and that all other modes begin and remain unexcited. The model system consistent with these assumptions has the form

$$\frac{d^2 Z_1}{d\tau^2} + (A_1 + C|Z_2|^2)\, Z_1 = U_1 \qquad (14)$$

$$\frac{d^2 Z_2}{d\tau^2} + (A_2 + C|Z_1|^2)\, Z_1 = U_2$$

From Figure 4a we have the correspondence

$$A_j = \omega^2 (\vec{k}_j, \alpha)$$

$$C = \frac{\beta}{3N^2} |\vec{k}_1 \times \vec{k}_2|^4 \left(|\vec{k}_1 + \vec{k}_2|^{-4} + |\vec{k}_1 - \vec{k}_2|^{-4}\right)$$

In order to study the system of equations (14) the explicit values of β, N, $\vec{k}_1$, $\vec{k}_2$ and α are not needed, so long as the A_j and C are non-negative. It should be noted that (14) are in general complex; however, since $Z(\vec{k}, t) = Z^*(-\vec{k}, t)$, the complex conjugates of (14) are not independent of (14) themselves, and the two (complex) equations of (14) are thus the complete set of system equations.

Since the Z_i are generally complex, the two explicit equations in (14) are implicitly four. However, if the Z_i are assumed to be each either fully real or fully imaginary, then there are only two equations; this then is the smallest reduction of the von Karman system of equations which remains nonlinear: two equation in two unknowns.

These two, coupled nonlinear equations can represent a real physical system if $Z_1 = i R_1$, $Z_2 = i R_2$ ($i = \sqrt{-1}$; R_j: real). The system then corresponds to a simply supported vibrating plate, the situation considered by Crawford and Atluri. The system of equations (14) becomes

$$\frac{d^2 R_1}{d\tau^2} + (A_1 + C R_2^2) R_1 = U_1 \qquad (15a)$$

$$\frac{d^2 R_2}{d\tau^2} + (A_2 + C R_1^2) R_2 = U_2 \qquad (15b)$$

This basic system can now be studied to gain some insight into the nature of a more complex multi-mode system.

To begin, if (15a) is multiplied by $dR_1/d\tau$ and (15b) by $dR_2/d\tau$, there results the following two equations:

$$\frac{d}{d\tau}\left[\frac{1}{2}\left(\frac{dR_1}{d\tau}\right)^2 + \frac{1}{2} A_1 R_1^2\right] + \frac{1}{2} C R_2^2 \frac{dR_1^2}{d\tau} = U_1 \frac{dR_1}{d\tau} \qquad (16a)$$

$$\frac{d}{d\tau}\left[\frac{1}{2}\left(\frac{dR_2}{d\tau}\right)^2 + \frac{1}{2} A_2 R_2^2\right] + \frac{1}{2} C R_1^2 \frac{dR_2^2}{d\tau} = U_2 \frac{dR_2}{d\tau} \qquad (16b)$$

If this system is linear, $C = 0$; furthermore, if there is no forcing, $U_1 = U_2 = 0$ and the following quantities are individually conserved ($k = 1,2$):

$$\xi_k = \frac{1}{2}\left[\left(\frac{dR_k}{d\tau}\right)^2 + A_k R_k^2\right] \qquad (17)$$

The ξ_k ($k = 1,2$) are the 'linear' energies of the two modes. Now, suppose $C \neq 0$ but $U_1 = U_2 = 0$; ξ_1 and ξ_2 are no longer individually conserved, but a single conserved quantity still exists, for if (16a) and (16b) are added together the result is

$$\frac{d}{d\tau}\left(\xi_1 + \xi_2 + \frac{1}{2} C R_1^2 R_2^2\right) = U_1 \frac{dR_1}{d\tau} + U_2 \frac{dR_2}{d\tau} \qquad (18)$$

If the modal control forces U_1 and U_2 are zero the total energy of the system $\xi = \xi_1 + \xi_2 + \frac{1}{2} C R_1^2 R_2^2$ is obviously conserved.

The system of equations (15a, b) can be easily solved numerically; this was done using the same time-stepping scheme as for the multimode system ($\Delta\tau = 0.01$) although here the nonlinear terms are evaluated directed (no transfrom). This was done using the same time integration scheme as for the multi-mode case, with a dimensionless time-step of 0.01; here, the nonlinear terms were evaluated directly, rather than by transform. As an example, let $A_1 = 1.0$, $A_2 = 2.0$ and $C \in \{0, 1/4, 1/2, 1, 2, 4, 8, 16\}$; this procedure allows the behavior of the system to be studied as the nonlinearity is increased. The results are shown in Figures 7a-h; notice that although ξ is conserved, ξ_1 and ξ_2 are not, as C increases in value. Energy is apparently being transferred between the two modes through their mutual non-linear coupling.

In Figure 8 another interesting aspect of the dynamics is revealed; there, a comparison is given between the temporal behavior of the total energy ξ and the sum of individual linear energies ξ_1 and ξ_2. Notice that $\xi_1 + \xi_2 \neq \xi$ in general; i.e., there also exists a 'non-linear' energy of coupling between the modes which fluctuates between zero and roughly half of the total energy. In Figure 8 we see that the non-linear coupling energy goes through many fluctuation cycles as energy is being shifted back and forth between modes. In contrast consider Figure 6; there the multi-mode system has apparently not even gone through one fluctuation cycle, suggesting that most of the interesting dynamical history remains to be explored (given sufficient computer resources).

Control

The minimal nonlinear system described in this chapter was used to study the effect of a linear control law on a structure which was inherently nonlinear, as this situation may occur in practice. The discrete control law chosen was that of Williams and Montgomery[13] which uses the two most recent past values of displacement and control inputs to calculate the new control inputs at each time step. The fact that this controller uses two past values of displacement implies the presence of rate feedback; this is important because it is evident from (18) that modal control inputs opposite in sign and proportional to the instantaneous modal rates will always decrease the total energy (the 'Lyapunov' function of the system).

The characteristic equation of the system with the controller of Williams and Montgomery has four roots. Here, it was assumed that these were two pairs of conjugate roots; the real and imaginary parts of one pair were both equal to 0.3535 and $\pm$ 0.3535, respectively, while the other pair had real and imaginary parts of 0.4949 and $\pm$ 0.4949, respectively. This placed the roots well inside the unit circle in the complex plane, ensuring stability. Using this control scheme, the nonlinearity parameter C in (15a,b) was set to a number of values, starting with zero, to examine the effect of increasing the nonlinearness of the system on the controller. The sampling time was, in dimensionless units, 0.20.

The behavior of the amplitudes R_1 and R_2 of (15a,b) are shown in Figures 9, 10, 11, and 12. In Figure 9 and 10, the system parameters are $A_1 = 1$, $A_2 = 2.25$, $C = 0$: the system is linear, the modes are uncoupled and damp out smoothly. In Figures 11 and 12, $A_1 = 1$, $A_2 = 2.25$ and $C = 8$: the system is highly non-linear, the behavior is initially erratic, but still damps out, though not as quickly as when $C = 0$. Notice that during the initial erratic phase, the oscillations of both R_1 and R_2 do not have zero mean. (Figures 9 and 10, the ideal responses of a linear system, should be compared with Figures 11 and 12, respectively, the actual responses of the nonlinear system.)

This result indicates that although the dynamic response of the nonlinear system to linear control is erratic at first, the system is ultimately controlled. It would be interesting to study this phenomenon further, particularly on the multi-mode system discussed in the previous chapter. In so doing, the presence of spillover could be investigated, a problem which is explicitly avoided in the minimal nonlinear system. The effect of nonlinearities on desired controller response, along with other interesting topics, could also be examined (provided the computational resources are available).

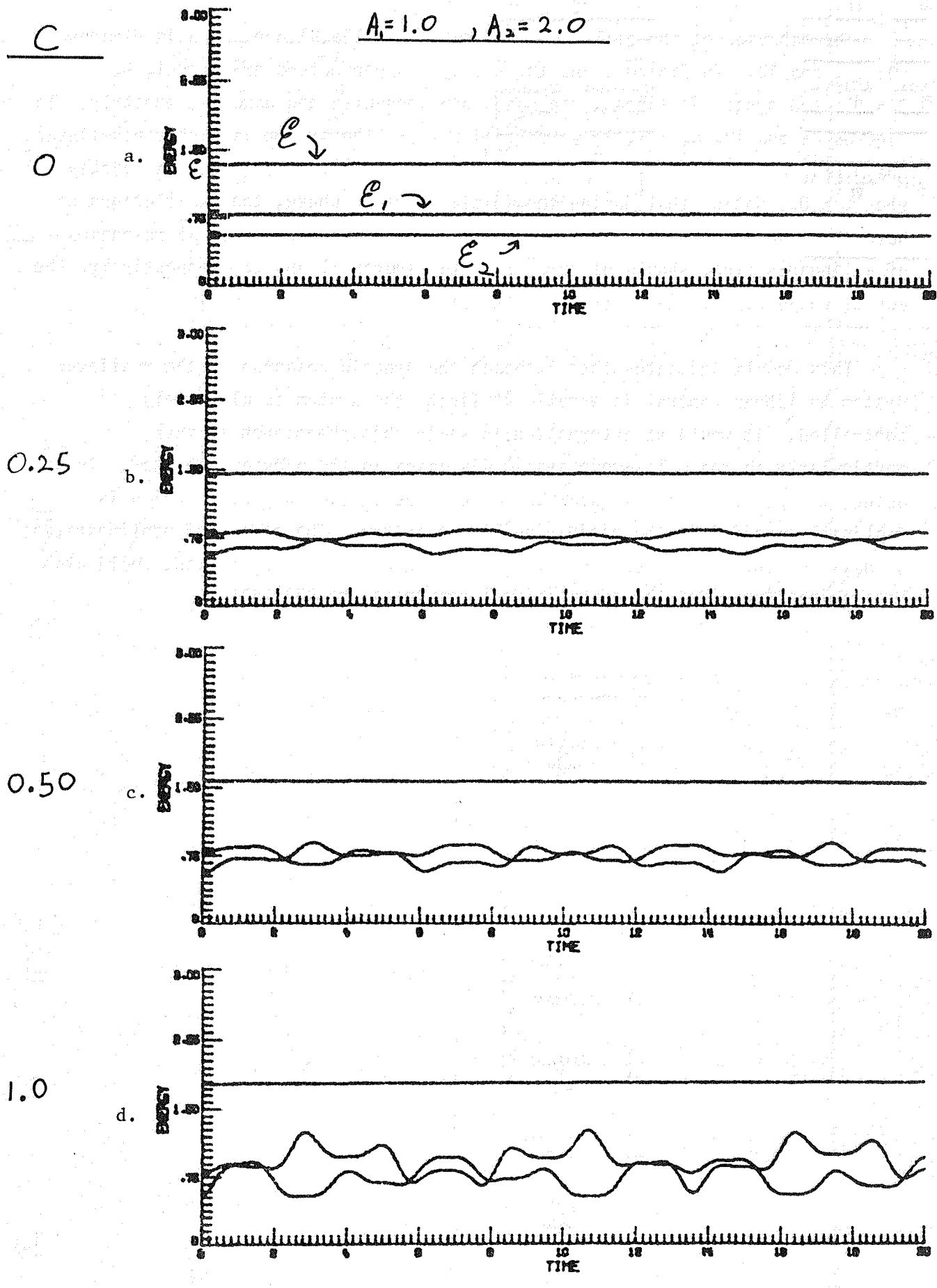

FIGURE 7. LINEAR AND TOTAL ENERGIES OF A TWO MODE SYSTEM.

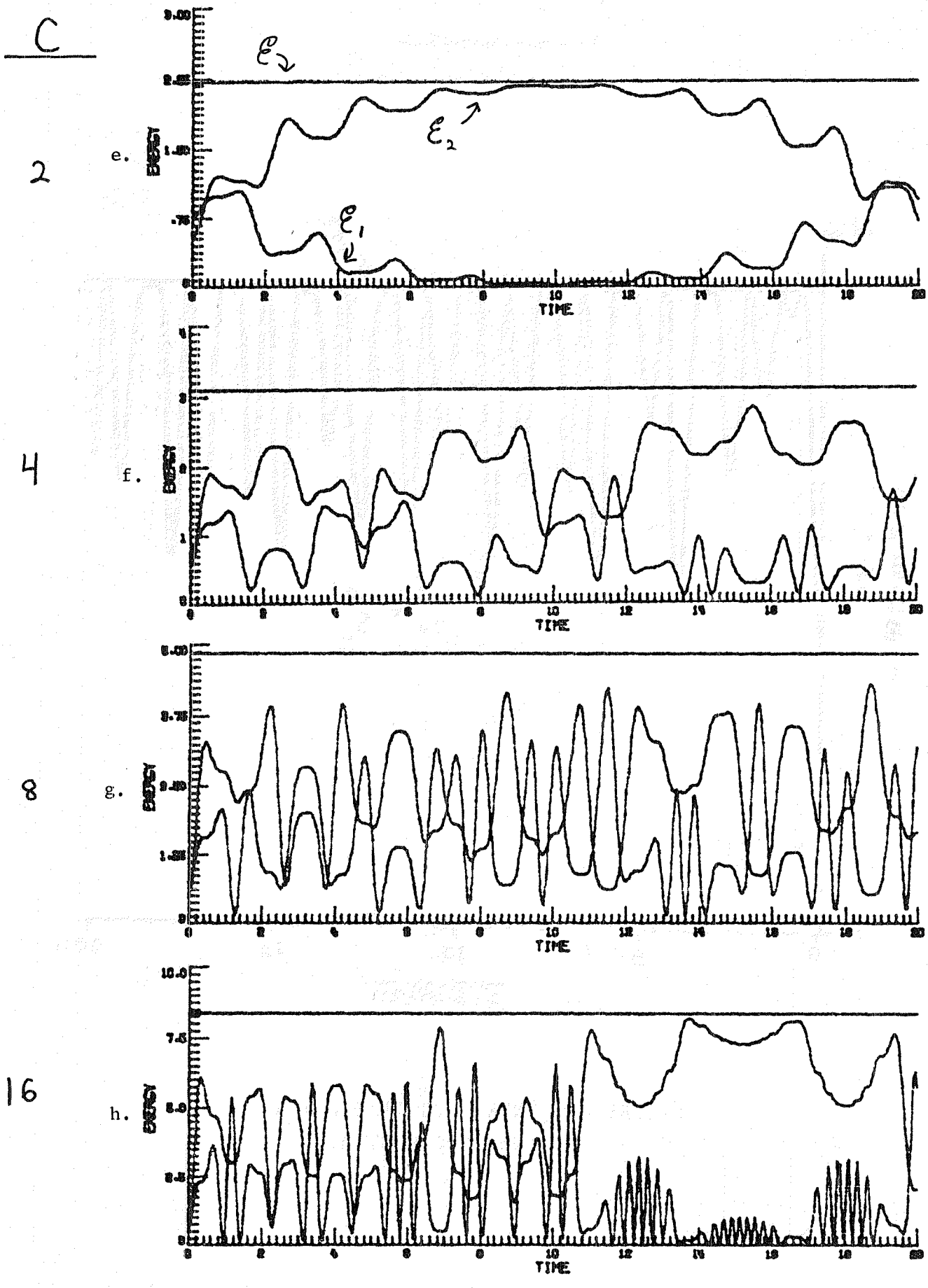

FIGURE 7. LINEAR AND TOTAL ENERGIES OF A TWO MODE SYSTEM.

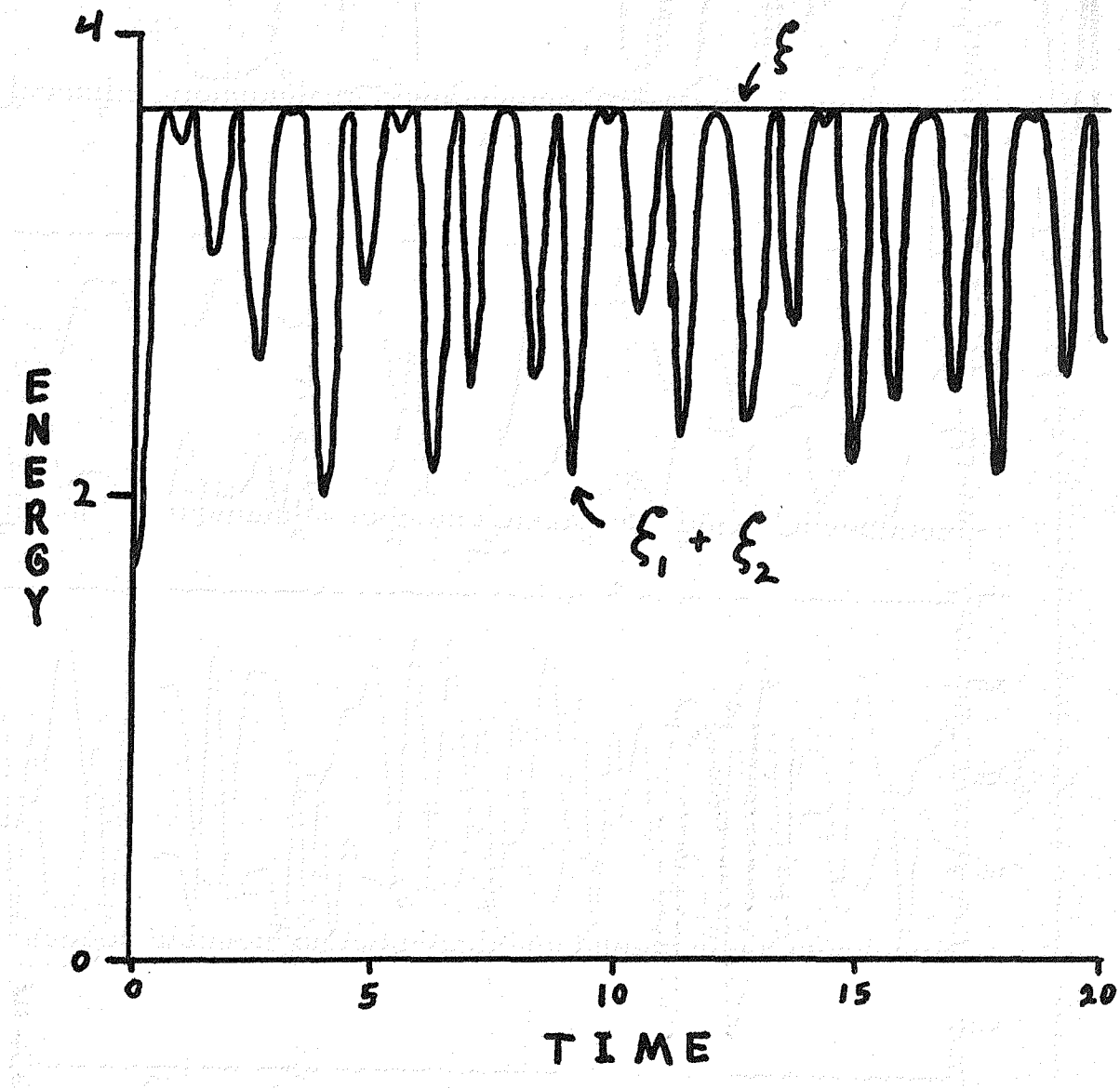

FIGURE 8. ENERGY VS TIME FOR A TWO MODE SYSTEM.

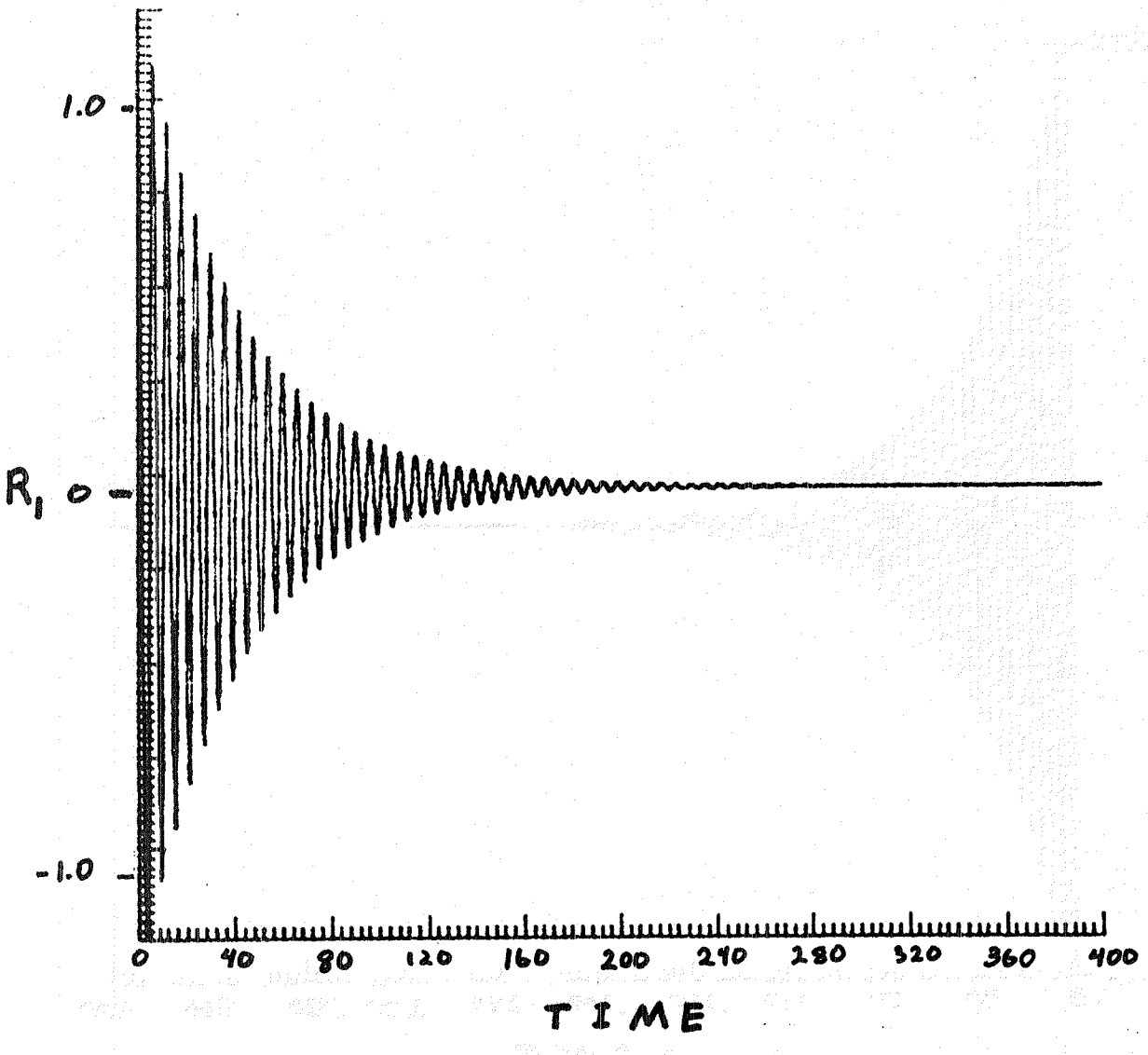

FIGURE 9. TIME DEPENDENCE OF R_1
FOR $A_1 = 1$, $A_2 = 2.25$, $C = 0$

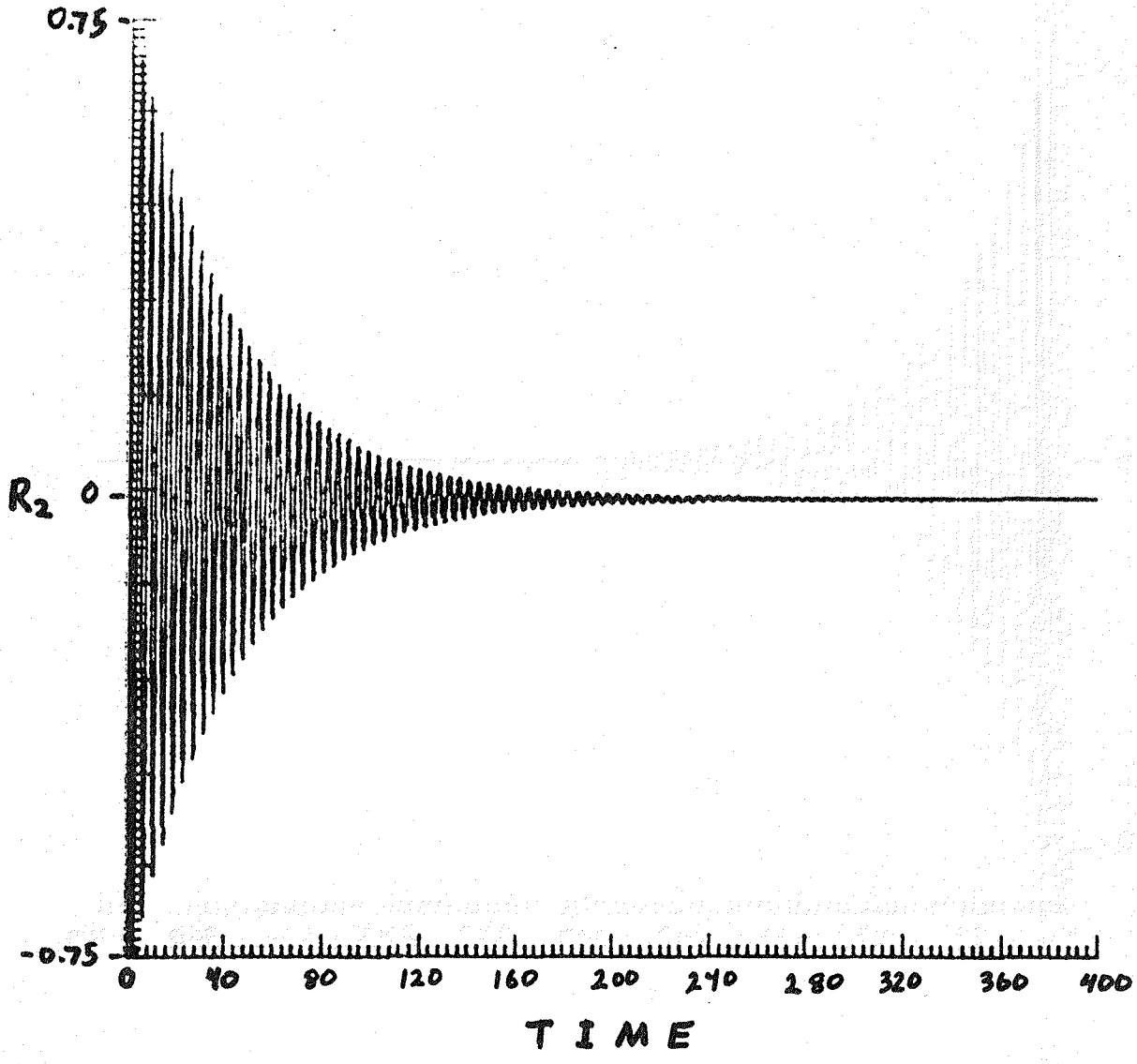

FIGURE 10. TIME DEPENDENCE OF R_2
FOR $A_1 = 1$, $A_2 = 2.25$, $C = 0$

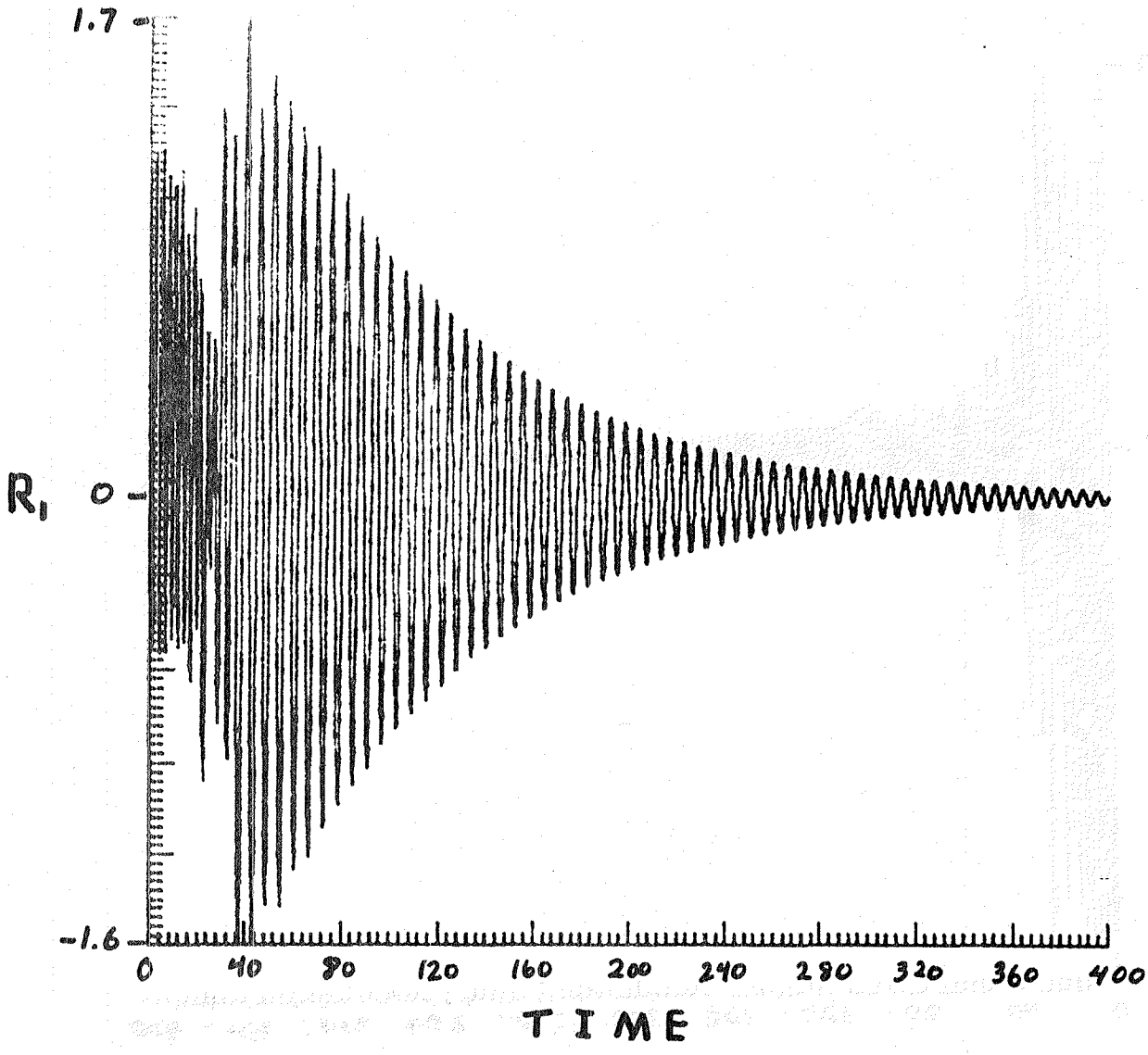

FIGURE 11. TIME DEPENDENCE OF R_1 FOR $A_1 = 1$, $A_2 = 2.25$, $C = 8$.

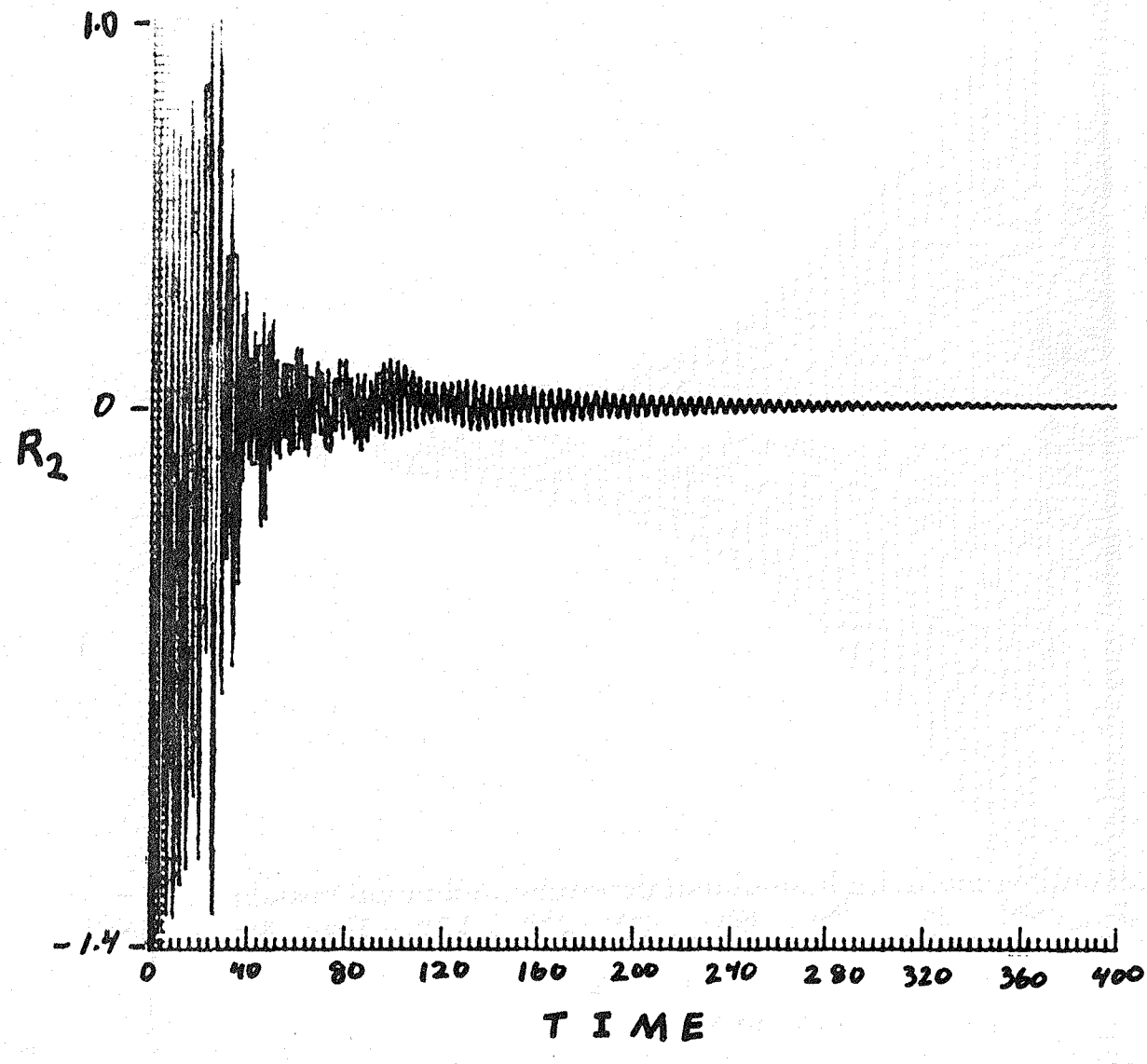

FIGURE 12. TIME DEPENDENCE OF R_2
FOR $A_1 = 1$, $A_2 = 2.25$, $C = 8$.

CHAPTER 7
SUMMARY

In this report the nonlinear dynamics and control of a vibrating rectangular plate were investigated. The dynamics of the plate were simulated by solving the von Karman equations through the use of an Orszag-Patterson type Fourier spectral transform method. Although arbitrary boundary conditions could be implemented by using Lanczos' Tau Method, this was not done due to the lack of computer resources.

In order to overcome the computational cost inherent in a full-blown, multi-mode simulation, a reduced order model was studied. This reduced model was a minimal von Karman system: two coupled nonlinear differential equations in two unknowns. This minimal set contained all the qualitative details of a multi-mode simulation: nonlinear coupling and the presence of a Lyapunov function. Preliminary results indicate that controllers with at least implicit rate feedback, even if predicated on a linear modeal, can eventually control and dampen the nonlinear oscillations, as long as the nonlinear terms are not too dominant.

The minimal and the multi-mode systems discussed herein can be profitably used to study a number of interesting problems. Different control laws can be studied using either the minimal or multi-mode system as the plant; in the minimal system, spillover is explicitly avoided, while in the multi-mode system its full effects can be investigated. Lyapunov theory can also be applied in more detail to these nonlinear systems to help shed light on questions of control.

Additional problems of interest include the relation between modal autocorrelation time and control system sampling rate, and the phase space structure of both the conserved and damped nonlinear dynamic system. (Other nonlinear systems have already been shown to possess interesting and unexpected dynamic behavior[15]).

The end to which this research is directed is, of course, to understanding and controlling the dynamics of real-world systems. Amongst these are large space structures, fluttering wings and other extended, relatively flimsy structures of interest to NASA. As these structures are difficult to experimentally simulate on the earth's surface, and since we would like to know as much as possible before putting these objects into orbit, a numerical simulation provides a viable alternative with which to gain the requisite knowledge.

REFERENCES

1. L. D. Landau and E. M. Lifshitz: Theory of Elasticity, Pergamon, Oxford, 1970.

2. A. E. H. Love: A Treatise on the Mathematical Theory of Elasticity, Dover, New York, 1944.

3. J. J. Stoker, Nonlinear Elasticity, Gordon and Breach, New York, 1968.

4. D. Gottlieb and S. A. Orszag: Numerical Analysis of Spectral Methods: Theory and Applications, SIAM, Philadelphia, 1977.

5. E. Turkel: Numerical Methods for Large-Scale, Time-Dependent Partial Differential Equations, ICASE Report 79-20, NASA/LaRC, Hampton, Virginia, 1979.

6. S. A. Orszag, Stud Appl. Math., 50, 293, 1971.

7. G. S. Patterson and S. A. Orszag, Phys. Fluids, 14, 2538, 1971.

8. Gottieb and Orszag, op.cit. (ref.4), p. 11.

9. R. H. Kraichnan and D. Montgomery, "Two-dimensional Turbulence," Rep. Prog. Phys., 43, pp. 547-619, 1980.

10. L. D. Landau and E. M. Lifshitz, Statistical Physics, 3rd ed., pp. 11-14, 79-82, Pergamon, New York, 1980.

11. J. Crawford and S. Atluri, J. Sound and Vibr., 43, pp. 117-129, 1975.

12. D. Potter, Computational Physics, p. 34, John Wiley, New York, 1973.

13. J. P. Williams and R. C. Montgomery, "Simulation and Testing of Digital Control on a Flexible Beam," AIAA Guidance and Control Conference, 1982.

14. B. C. Kuo, Digital Control Systems, pp. 287-294, Holt, Rinehart and Winston, New York, 1980.

15. R. H. G. Helleman, "Self-Generated Chaotic Behavior in Nonlinear Mechanics," in Fundamental Problems in Statistical Mechanics, pp. 165-233, E. G. D. Cohen, ed., North Holland, New York, 1980.

1. Report No.	2. Government Accession No.	3. Recipient's Catalog No.
NASA CR-172215		

4. Title and Subtitle	5. Report Date
Nonlinear Dynamics and Control of a Vibrating Rectangular Plate	October 1983
	6. Performing Organization Code
7. Author(s)	8. Performing Organization Report No.
John V. Shebalin	
	10. Work Unit No.
9. Performing Organization Name and Address Kentron International, Inc. Kentron Technical Center 3221 Armistead Avenue Hampton, Virginia 23666	11. Contract or Grant No. NAS1-16000
	13. Type of Report and Period Covered Contractor Report
12. Sponsoring Agency Name and Address National Aeronautics and Space Administration Washington, D.C. 20546	14. Sponsoring Agency Code

15. Supplementary Notes

Langley Technical Monitor: Raymond C. Montgomery

16. Abstract

The von Karman equations of nonlinear elasticity are solved for the case of a vibrating rectangular plate by means of a fourier spectral transform method. The amplification of a particular Fourier mode by nonlinear transfer of energy is demonstrated for this conservative system. The multi-mode system is reduced to a minimal (two mode) system, retaining the qualitative features of the multi-mode system. The effect of a modal control law on the dynamics of this minimal nonlinear elastic system is examined.

17. Key Words (Suggested by Author(s))	18. Distribution Statement
Nonlinear elasticity Fourier analysis Control Theory	Unclassified-Unlimited Subject Category 39

19. Security Classif. (of this report)	20. Security Classif. (of this page)	21. No. of Pages	22. Price
Unclassified	Unclassified	40	A03

For sale by the National Technical Information Service, Springfield, Virginia 22161

End of Document